ABILITY OF NEAR INFRARED SPECTROSCOPY TO MONITOR AIR-DRY DENSITY DISTRIBUTION AND VARIATION OF WOOD

Brian K. Via†
Ph.D. Graduate

Chi-Leung So†
Post Doctoral Researcher

Todd F. Shupe†
Associate Professor

Michael Stine
Associate Professor
School of Renewable Natural Resources
Louisiana State University AgCenter
Baton Rouge, LA 70803

and

Leslie H. Groom†
Project Leader
USDA Forest Service
Southern Research Station
Pineville, LA 71360

(Received February 2004)

ABSTRACT

Process control of wood density with near infrared spectroscopy (NIR) would be useful for pulp mills that need to maximize pulp yield without compromising paper strength properties. If models developed from the absorbance at wavelengths in the NIR region could provide density histograms, fiber supply personnel could monitor chip density variation as the chips enter the mill. The objectives of this research were to a) develop density histograms from actual density versus density histograms developed through NIR modeling, and b) determine the precision of density models developed from absorbance in the NIR region with a recommendation for the sample size needed to estimate the standard deviation of density at a given precision.

Models for density were developed from calibration samples ($n = 170$) and then validated with 93 randomly held aside samples. The samples were systematically removed from 10 longleaf pine trees of equal age, but different growth rates. The histogram patterns for actual density almost paralleled the histogram patterns developed from predictive models. Subsequently, the validation data set was randomly categorized into groups of three, and the standard deviations of density were measured. For three measurements per data point, the predicted standard deviation covaried with the actual standard deviation of density with an $R^2 = 0.61$ and 0.55 for the calibration and validation data set, respectively. A sample size of 30 was recommended to estimate the standard deviation of density with a precision of 0.01 g/cm^3.

Keywords: Chip, density, near infrared spectroscopy (NIR), wood, pine, statistical process control, pulp yield.

† Member of SWST.

INTRODUCTION

Wood density is the most important factor affecting pulp and wood quality (Kleppe 1970; Kibblewhite 1984; Duffy and Kibblewhite 1989). Being able to monitor the density of the raw material going into the mill is, perhaps, the next crucial step in improving efficiency for pulp and paper manufacturers. The pulp and paper industry places a high importance on lowering the variation of any variable that will decrease costs with density being important (Kleppe 1970). While many technological improvements have been made over the decades, there is still one inherent variation to overcome, the material itself. This paper evaluates the ability of near infrared spectroscopy (NIR) to monitor wood density.

For paper products, an increase in density will increase pulp yield and tear index, but will decrease tensile, burst, apparent density, and stretch (Duffy and Kibblewhite 1989; Kibblewhite et al. 1997). Since increased density will bring about a compromise in paper strength, Kleppe (1970) suggested that density should be improved for increased pulp yield as long as an acceptable level of strength is maintained. For example, linerboard can utilize high density southern pine chips while maintaining an acceptable burst index (Kleppe 1970).

The increase in pulp yield with increased density is caused by the higher concentration of cellulose in latewood and the additional porosity of the earlywood zone (Gladstone et al. 1970; Labosky and Ifju 1972). Differences in the magnitude of porosity between latewood and earlywood result in uneven rates of liquor penetration and thus pulp yield, especially for shorter cooking periods (Labosky and Ifju 1972). Latewood can exhibit 2 to 7 percentage points higher yield than earlywood, setting the boundaries for pulp yield variation (Gladstone et al. 1970). As a result, density variation becomes a primary factor for most pulp and paper properties.

One mill study found density variation to double from one month to the next because of changing chip supply attributable to lack of control of mixing the right blend of species, but also natural variations in density within a species occur due to variations in log age (Farrington 1980). To solve this problem, efficient separation of topwood, slabwood, and corewood chips is suggested (Veal et al. 1987). Others support the segregation of species by age and growth rate, since the predictive power of these variables on fiber morphology and strength indices is high (Kärenlampi and SuurHamari 1997). Mills already blend sawmill pine chips, or pine chips from thinnings, with hardwood chips to achieve a target chip density. As a result, nonnormal distributions are likely to occur, making the mean density less useful. Some method to monitor this complex variation is needed so that adjustments can be made at the blending station. With such a method, a mill could monitor incoming chips to make sure that fiber supply is providing the density that was paid for. But perhaps most important, the variation in density could be lowered so that there are fewer over- and undercooked chips. Such process control capacity would result in fewer rejects from customers while optimizing the use of manufacturing resources.

Near infrared spectroscopy (NIR) is now used to estimate solid wood density with R^2 values between 0.70 to 0.95 (Hoffmeyer and Pedersen 1995; Schimleck et al. 2001a,b; Schimleck et al. 2002; Schimleck and Evans 2003; Schimleck et al. 2003b; Via et al. 2003). Pulp yield can also be modeled with success through partial least squares regression (Michell and Schimleck 1998). However, by using the area under the spectra curve (absorbance of light at each wavelength in the near infrared range) as an independent predictor of density, a more robust model can be developed for both juvenile and mature wood (Via et al. 2003). Gindl et al. (2001) also found the average absorbance from every wavelength in the NIR region, to correlate with density. Manufacturing research shows NIR to predict lumber stiffness from density although later research cautions against using NIR to stress grade wood originating from the pith (Meder et al. 2003; Thumm and Meder 2001; Via et al. 2003).

Manufacturers also need to be able to measure

the wood density across a range of species, moisture content, and temperature. For 54 species, multivariate equations built from NIR spectra can be used to estimate density, with high accuracy. (Antti et al. 1996; Schimleck et al. 2001a; Schimleck et al. 2003). It is also possible to classify wood to a species before predicting density (Schimleck et al. 1996; Tsuchikawa et al. 2003). Such a procedure may help to decide which density calibration equation to use for different species.

Moisture may be an additional variable to add noise to absorbance response. Hoffmeyer and Pedersen (1995) found wood density prediction to be reasonably independent of moisture content below fiber saturation point (FSP). Above FSP, robust calibration models for many chemical and physical properties of chips can be built when moisture is allowed to vary (Axrup et al. 2000). Also, during calibration, removal of hydroxyl-associated wavelengths can result in more robust calibration equations for density (Swierenga et al. 2000). If temperature varies, as in a manufacturing environment, then one needs to account for the temperature by either removing temperature-sensitive wavelengths before calibration or include the full range of temperature into the design of model development (Thygesen and Lundqvist 2000; Wülfert et al. 2000).

Absorbance in the NIR region may thus be an applicable independent variable for measuring the density distribution of wood. NIR absorbance is currently being monitored for other wood properties in a manufacturing environment. For example, histograms of estimated lignin can be successfully plotted to monitor online variation and distribution (Jääskeläinen et al. 2003).

While not the objective of this experiment, success at measuring density variation from NIR signal would provide a tool to control the variation of chip density going into the mill. For this experiment, the absorbance in the NIR range was restricted to the radial face of wood, under controlled temperature and moisture content, with a fixed distance between the probe and the wood sample, and with negligible variation in sample dimensions. For an industrial setting, all these factors will vary, and the proper inclusion of this multiple variation is necessary when building calibration equations. Jonsson et al. (2004) provides a detailed experimental design for manufacturers to capture such variation and would be applicable to the calibration of chip density.

For this paper, the objective was to determine the ability to use absorbance from the NIR region to predict the variation in air-dry density of solid wood in tightly controlled laboratory conditions. Thus, histograms of actual density were compared to histograms from predicted density. Also, density standard deviations were compared with NIR-estimated standard deviations of density. Finally, the ability of NIR to classify solid wood into density categories was investigated.

METHODS

Ten longleaf pine (*Pinus palustris*) trees 41 years old were selected from a plantation on the Harrison Experimental Forest, which is owned and maintained by the USDA Forest Service (Saucier, MS). Three trees of small diameter, three trees of large diameter, and four trees in the medium diameter range were randomly selected. The location was 30.6° north and 89.1° west. Prescribed fires were applied periodically to the understory for the entire life of the stand to keep down unwanted understory vegetation. Trees were planted 3.66 m apart from neighboring trees in an equilateral triangle pattern, with one border row surrounding the site. Each of the 10 trees was harvested and cut into bolts every 4.57 m in height, yielding 5 to 7 bolts. Each bolt had an accompanying disk cut from the basal end of the bolt. The specimens for density measurement were taken from the bolt while the spectra were acquired from the radial face of a strip ripped from the adjoining disk. The spectra acquisition was taken within 30 mm of the actual density measurement and at the same age. Specimens for density measurement were taken at rings 1, 4, 8, 16, 32, and the last ring of each disk. Since the number of rings decreases up the

stem, not all of these rings were available at each height. The volume for air-dry density (8.1% moisture content) was measured with calipers, and the weight was measured at equilibrium moisture content (EMC). The EMC had a mean of 8.1% and a standard deviation of 1.6%. Dimensions were measured to the nearest 0.0025 cm, while weights were measured to the nearest 0.001 g.

NIR absorbance was obtained using a Nexus 670 FTIR spectrometer (Thermo Nicolet Instruments, Madison, WI). Scans were acquired at 1-nm intervals between the wavelengths of 1000 and 2500 nm. Forty scans were collected and averaged into one spectrum. During NIR scanning, the temperature was controlled at 22C° ± 1 with a mean relative humidity of 50%. The samples were laid on a flat surface under a light source and positioned such that the center latewood portion of the ring was in the center of the 5-mm-diameter spot-sized beam.

To reduce data set and computation time, the spectra was reduced to 10-nm intervals by averaging (Schimleck et al. 2004). One hundred seventy samples were used to develop whole tree models while ninety-three samples were set aside for validation model building. In a separate report, multiple linear regression models and principal components regression showed slightly higher R^2 values of 0.75, but the area under the spectra curve provided an interpretable model and was used for this study (Via et al. 2003).

For data analysis, a linear model was developed predicting density from the area under the spectra curve. Frequency distribution histograms were developed for actual and predicted data. For standard deviation estimation, the samples were randomly clustered into groups of three, and standard deviations in density were computed from the actual and predicted data.

RESULTS AND DISCUSSION

Model validation

Multiple linear regression of selected wavelengths and principal components regression yielded the best R^2 values. However, since the spectra shifted upward as density increased, the following model was chosen:

$$D = 0.0008 * A + 0.1891 + \varepsilon \quad (1)$$

where D is the density, A is the area under the curve, and ε is error. An R^2 value of 0.71 was calculated when the actual density and predicted density were regressed (Fig. 1). Equation (1) exhibited better fits throughout the density range than other preliminary models. The fit was superior if the residuals around the regression line fell at equal variance throughout the density range and a mean of zero. Overfitting was determined to occur when the residuals around the predicted density did not randomly and normally distribute around zero for the validation data set. Overfitting may be defined as the instance where too many factors or independent variables were used to estimate the dependent variable density resulting in an inflated R^2 value and bias in the prediction of density in future populations. Table 1 presents the summary statistics when predicting density from the area under the spectra curve.

Equation (1) was important because it may encourage other researchers to follow a similar approach. The coefficient and intercept of many commercially important species would be useful information and may provide universal equations although machine differences would have to be taken into account.

Excessive extractives were often present nearby the pith. The additional extractives increased apparent density by adding additional

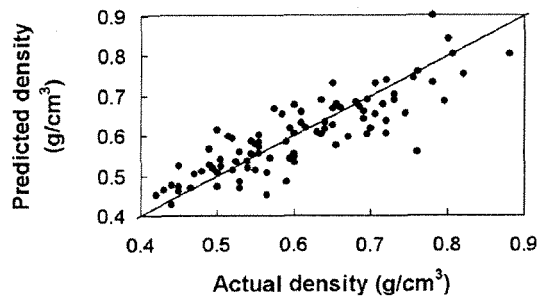

FIG. 1. Regression analysis plot of air-dry density from the area under the spectra curve versus actual density (n = 170).

TABLE 1. *Summary statistics for density model and model distribution.*

	Sample size	R^2	RMSE	Distribution mean density	Distribution kurtosis	Distribution skewness
Calibration	170	0.71	0.052	0.59	0.546 s	0.690 s
Validation	93	0.69	0.055	0.60	0.298 ns	0.626 s

Note: s represents significant kurtosis or skewness while ns represents non-significance.

mass for a given volume of wood. At the same time, the area under the curve increased dramatically near the pith due to excessive extractives (Via et al. 2003). It was thus suspected that ring 1 may not be appropriate for inclusion in the calibration data set. While this paper did not extract the wood samples, such information may be ambiguous for those interested in density variation attributable to the cell wall. However, when ring 1 data was removed from the calibration data set to avoid excessive extractives, no significant differences in models occurred. Therefore, models encompassing ring 1 were included during the calibration stage.

Distribution modeling

Distribution properties were first considered for the calibration data. Histograms were developed from the actual density and compared to the density predicted in Eq. (1). As seen in Fig. 2a, the histograms for both actual density and NIR-predicted density deviated from the normal Gaussian. The slightly lower variation in the density predicted from Eq. (1) was probably attributable to the central limit theorem, which states that the variation in means is lower than the variation in the actual data that comprised the means (Freund and Walpole 1980). Since Eq. (1) predicts the mean density for a given absorbance, the predicted density variation was expected to be lower than the actual density variation. The shape and variance of the actual and predicted density were quite similar. To test the legitimacy of Eq. (1), validation data from 93 hold-out samples were computed and compared (Fig. 2b).

The histogram of the predicted and actual density data, for the validation data, was almost identical (Fig. 2b). A small shift in wood density was apparent between the actual and predicted

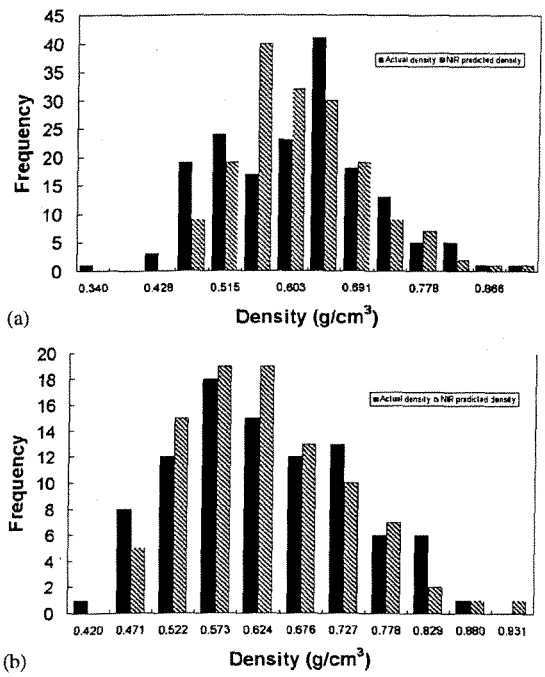

FIG. 2. Histograms for actual and predicted density for (a) calibration (n = 170) and (b) validation data (n = 93).

data values (Fig. 2b). In other words, the NIR model histogram appeared to slightly overestimate density as apparent from the shift toward higher density values. This did not occur in the calibration data, suggesting a slight bias in the model caused by random noise in selection of the validation samples. Another noteworthy point was the change in distribution shape when going from Figure 2a to 2b. The model output was mildly skewed to the right with the same variance as the actual data (Fig. 2b). It should also be noticed that the NIR calibration overpredicted some of the lower density samples for validation data set (Fig. 2a and b). Since the lowest density material commonly occurred near the pith and excessive extractives were common

in this region, perhaps local variations in extractives content near the beam resulted in overestimation of density. As explained earlier, excessive extractives were apparent to the eye near the low density pith and the corresponding spectra increased in mean absorbance by some unquantified amount resulting in an increase in the area under the spectra curve. However, it should be reiterated that removal of the ring 1 data from the calibration set did not change model predictions, perhaps due to a low sample size of data from the pith wood region.

Being able to measure skewness or even bimodal distributions would prove useful in manufacturing. For example, if the distribution is skewed right, a pulp mill may adjust for the median density instead of the mean. For other applications, such as lumber drying, the kiln-drying schedule may be adjusted to ensure that no pieces of lumber are above the required 19% in moisture content.

For Fig. 2a and b, both distributions were positively skewed as determined by statistical tests reported in Tabachnick and Fidell (1996) (Table 1). The skewness was attributable to the higher counts of high density rather than low density samples. Since density increased from pith to bark, there were more high than low density samples resulting in a skewed distribution.

By plotting out density histograms, manufacturers would be able to notice subtle or large changes in material variability. Currently, many pulp manufacturers are reluctant to consider categorizing their logs by age, height, or both, since such practices would require a heavy process change and financial capital. However, in New Zealand and Australia, such innovative practices are helping to make pulp and forest product manufactures more efficient by lowering the variation in final product properties. Such a visual plot may encourage more inefficient mills to classify their raw material in the log yard in an attempt to lower or control density variation.

It should be noted that this experiment was performed in the confines of a laboratory with a low wood moisture content and temperature range. In a manufacturing environment, the moisture will vary widely and may be above FSP. Any model developed by a mill should incorporate the complete range of temperature and wood moisture content in their calibration equation (Thygesen and Lundqvist 2000; Wülfert et al. 2000; Jonsson et al. 2004).

Dispersion modeling

Mapping out complete distributions may require significant computing resources. It may be more useful to consolidate the data into a variance or standard deviation estimate. The variation in density will probably lower if a batch of similarly aged logs are processed at the same time, and could be detected through a standard deviation estimate. In a pulp mill, it is not uncommon for a truck load of similarly aged logs to be stacked and processed together, resulting in wide shifts in material density from day to day.

Figure 3a demonstrates the ability to model the standard deviation of density from Eq. (1).

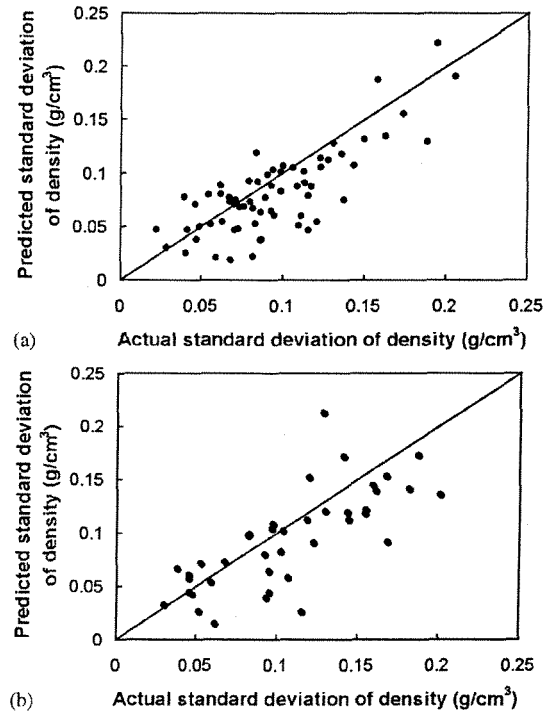

FIG. 3. Actual standard deviation for samples grouped into threes versus that predicted by NIR models (a) calibration (n = 170) and (b) validation data (n = 93).

Using 3 replicates to determine a single point, an R^2 of 0.61 was found between the actual density and that predicted by Eq. (1). Since only three samples were used to calculate each data value for the actual and predicted density, a higher R^2 may be possible in a manufacturing environment where more scans are possible.

Figure 3b demonstrates the ability of Eq. (1) to model the standard deviation of density for the validation data. A slightly lower $R^2 = 0.55$ was observed when the NIR predicted standard deviations were regressed against the actual standard deviations of density. It was interesting to notice that both Figs. 3a and 3b exhibited more data points on the bottom side of the 1:1 line than on the upper end, an indication of bias due to the slight deviation from normality as shown in Table 1.

Figure 4 was constructed to estimate the sample size needed to closely assess the overall population standard deviation of density. Around 30 data points were needed to estimate the standard deviation to a ±0.01 precision. As can be seen in Fig. 4, many more data points were needed to improve the estimation of the population standard deviation below ±0.01 precision. Thus, one might develop a control chart using 30 samples to estimate a single density variance data point. A moving average may be used to remove any autocorrelation between samples collected in a short time span (Jonsson et al. 2004).

Figure 5 shows the distribution of the standard deviation to be heavily skewed right. Since the standard deviation can not drop below zero and the probability of lower values being higher was intuitive, a right-sided skew was expected. This non-normal property would need consideration when developing a control chart for density. Otherwise, false alarms could occur when the estimated standard deviation falls outside the 95% confidence limits as assumed under the normal distribution.

Discrimination of density

For some applications, it may be desirable to classify on-line chip density into a given set of classes instead of predicting a specific value. For example, a pulp mill may be satisfied with a low, medium, and high density classification given the wide range in density that may occur from tree to tree. This wide variation might occur if tree age is heterogeneous within the log yard or by the time a group of trees are processed.

Table 2 demonstrates the ability to classify according to the number of classes/partitions as a function of the full range of density. In this table, the range of density was between 0.35 to 0.9 grams per cubic centimeter. A partition of 2 resulted in a separation of low, medium, and high density. When this was done, 99% of the specimens were properly classified.

When going from 2 to 11 partitions, the percent correct classification column was expected

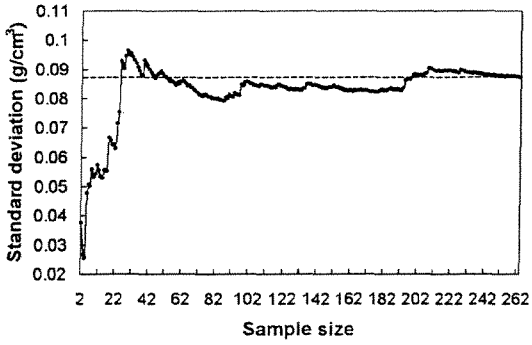

FIG. 4. *Sample size versus estimated standard deviation with the known standard deviation of the population plotted as a dashed line.*

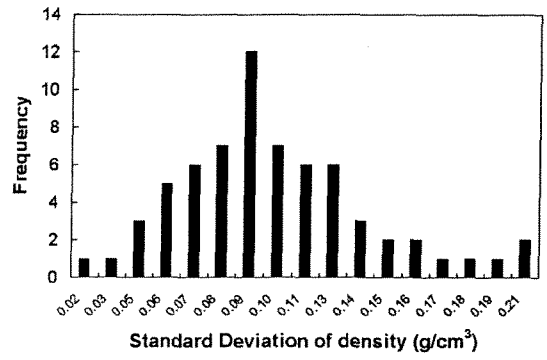

FIG. 5. Histogram of density standard deviations for all samples demonstrating the non-normal response.

TABLE 2. *The ability of NIR to classify wood density for different precision categories.*

Density increments g/cm^3	Number of partitions	Percent correct classification by NIR
0.250	2	99
0.167	3	91
0.125	4	89
0.100	5	74
0.083	6	89
0.071	7	72
0.063	8	76
0.055	9	76
0.050	10	67
0.045	11	78

to drop since the error remained constant while the defined range in each class dropped. The drop in percent classification did occur, but not as distinctly as expected (Table 2). The reason for the variability in the correct classification with increased partions was attributable to the change in boundaries as shown in the increment column of Table 2. Each time a new partition was added, the increment became lower and all the classes changed to a narrower range resulting in different class boundaries. Thus, what might be correctly classified under one partition scheme might fall in the error region for another partitioning scheme.

According to Table 2, when the density increments were lowered to 0.045 grams per cubic cm, approximately 70% correct classification occurred. This agreed well with the variation in residuals of actual versus predicted density which fell at 0.06 or ±0.03 g/cm^3, as determined by the 95% confidence interval.

One limitation to the precision estimate was the diameter of the NIR spot size. A 5-mm diameter light beam in the near infrared range was used. However, some of the latewood and earlywood rings were as small as 0.3 mm in thickness, especially in the 30- to 40-year-old ring region, as measured from the pith outward. A typical difference between early and latewood density was 0.45 g/cm^3. As a result, an error between what was measured gravimetrically and what was actually scanned occurred if even only a slight difference in proportion of latewood was introduced. Using a smaller spot size may thus yield improved R^2 when predicting density from the area under the spectra curve (Eq. 1).

SUMMARY AND CONCLUSIONS

The mapping of density histograms, as predicted from area under the absorbance response for a range of NIR wavelengths, was nearly equivalent to the actual density histograms for the calibration and validation data. When the ability to monitor the variation in a sequential manner was investigated, the use of NIR was successful at roughly estimating the variation with just three measurements and resulted in a precision of between 0.03 to 0.05 g/cm^3. A sample size of 30 was recommended to estimate the standard deviation of density with a precision of 0.01 g/cm^3. Any measurements greater than 30, yielded much smaller incremental improvement in precision for a given improvement in sample size.

These results were based on a tightly controlled moisture and temperature range. More work beyond the scope of this paper is recommended to determine the precision of measuring density above fiber saturation point. What was critical about this work was that Eq. (1) was based on a fundamental positive relationship between absorbance and density. Future research determining the coefficients and intercepts for various species may be useful in building a database of models. Also, this study was based on 10 longleaf pine trees from the same site. For better model accuracy, a larger sample size from a broad range of longleaf sites would be required.

ACKNOWLEDGMENTS

This study was funded by the USDA National Research Initiative Competitive Grants Program Agreement No. 2001-35103-10908. This paper (No. 04-40-0026) is published with the approval of the Director of the Louisiana Agricultural Experiment Station.

REFERENCES

ANTTI, H., M. SJÖSTRÖM, AND L. WALLBÄCKS. 1996. Multivariate calibration models using NIR spectroscopy on

pulp and paper industrial applications. J. Chemometr. 10(5–6):591–603.

AXRUP, L., K. MARKIDES, AND T. NILSSON. 2000. Using miniature diode array NIR spectrometers for analyzing wood chips and bark samples in motion. J. Chemometr. 14(5–6): 561–572.

DUFFY, G. G., AND R. KIBBLEWHITE. 1989. A new method of relating wood density, pulp quality, and paper properties. Appita J. 42(3):209–214.

FARRINGTON, A. 1980. Wood and digester factors affecting kraft pulp quality and uniformity. Appita J. 34(1):40–46

FREUND, J. E., AND R. E. WALPOLE. 1980. Mathematical statistics: 3rd ed. Prentice-Hall, Inc., Englewood Cliffs, NJ. 548 pp.

GINDL, W., A. TEISCHINGER, M. SCHWANNINGER, AND B. HINTERSTOISSER. 2001. The relationship between near infrared spectra of radial wood surfaces and wood mechanical properties. J. Near Infrared Spec. 9(4):255–261.

GLADSTONE, W. T., A. C. BAREFOOT, AND B. J. ZOBEL. 1970. Kraft pulping of earlywood and latewood from loblolly pine. Forest Prod. J. 20(2):17–24.

HOFFMEYER, P., AND J. G. PEDERSEN. 1995. Evaluation of density and strength of Norway spruce by near infrared reflectance spectroscopy. Holz Roh-Werkst 53(3):165–170.

JÄÄSKELÄINEN, A. S., M. NUOPPONEN, P. AXELSSON, M. TENHUNEN, M. LÖIJA, AND T. VUORINEN. 2003. Determination of lignin distribution in pulps by FTIR ATR spectroscopy. J. Pulp Pap. Sci. 29(10):328–331.

JONSSON, P., M. SJÖSTRÖM, L. WALLBÄCKS, AND H. ANTTI. 2004. Strategies for implementation and validation of on-line models for multivariate monitoring and control of wood chip properties. J. Chemometr. 18(3–4):203–207.

KÄRENLAMPI, P., AND H. SUURHAMARI. 1997. Classified wood raw materials for diversified softwood kraft pulps. Pap. Puu-Pap. Tim. 79(6):404–410.

KIBBLEWHITE, R. P. 1984. Radiata pine wood and kraft pulp quality relationships. Appita J. 37(9):741–747.

———, R. EVANS, AND M. J. C. RIDDELL. 1997. Handsheet property prediction from kraft-fibre and wood-tracheid properties in eleven radiate pine clones. Appita J. 50(2): 131–138.

KLEPPE, P. J. 1970. The process of, and products from, kraft pulping of southern pine. Forest Prod. J. 20(5):50–59.

LABOSKY, P., AND G. IFJU. 1972. A study of loblolly pine growth increments. Part II. Pulp yield and related properties. Tappi J. 55(4):530–534.

MEDER, R., A. THUMM, AND D. MARSTON. 2003. Sawmill trial of at-line prediction of recovered lumber stiffness by NIR spectroscopy of *Pinus radiata* cants. J. Near Infrared Spec. 11(2):137–143.

MICHELL, A. J., AND L. R. SCHIMLECK. 1998. Developing a method for the rapid assessment of pulp yield of plantation eucalypt trees beyond the year 2000. Appita J. 51(6): 428–432.

SCHIMLECK, L. R., AND R. EVANS. 2003. Estimation of air-dry density of increment cores by near infrared spectroscopy. Appita J. 56(4):312–317.

———, A. J. MICHELL, AND P. VINDEN. 1996. NIR spectroscopy and principal components analysis. Appita J. 49(5): 319–324.

———, R. EVANS, AND J. ILIC. 2001a. Application of near infrared spectroscopy to a diverse range of species demonstrating wide density and stiffness variation. IAWA J. 22(4):415–429.

———, ———, AND ———. 2001b. Estimation of *Eucalyptus delegatensis* wood properties by near infrared spectroscopy. Can. J. For. Res. 31(10):1671–1675.

———, ———, AND A. C. MATHESON. 2002. Estimation of *Pinus radiata* D. Don clear wood properties by near-infrared spectroscopy. J. Wood Sci. 48(2):132–137.

———, ———, AND J. ILIC. 2003b. Application of near infrared spectroscopy to the extracted wood of a diverse range of species. IAWA J. 24(4):429–438.

———, R. STÜRZENBECHER, P. D. JONES, AND R. EVANS. 2004. Development of wood property calibrations using near infrared spectra having different spectral resolutions. J. Near Infrared Spec.12(1):55–61.

SWIERENGA, H., F. WÜLFERT, O. E. DE NOORD, A. P. DE WEIJER, A. K. SMILDE, AND L. M. C. BUYDENS. 2000. Development of robust calibration models in near infra-red spectrometric applications. Anal. Chem. Acta 411(1–2): 121–135.

TABACHNICK, B. G., AND L. S. FIDELL. 1996. Using multivariate statistics: third edition. Harper Collins, New York, NY. 880 pp.

THUMM, A., AND R. MEDER. 2001. Stiffness prediction of radiata pine clearwood test pieces using near infrared spectroscopy. J. Near Infrared Spec. 9(2):117–122.

THYGESEN, L. G., AND S. O. LUNDQVIST. 2000. NIR measurement of moisture content in wood under unstable temperature conditions. Part 1. Thermal effects in near infrared spectra of wood. J. Near Infrared Spec. 8(3):183–189.

TSUCHIKAWA, S., K. INOUE, J. NOMA, AND K. HAYASHI. 2003. Application of near-infrared spectroscopy to wood discrimination. J. Wood Sci. 49(1):29–35.

VEAL, M. A., G. R. MARRS, AND M. JACKSON. 1987. Control over the quality of loblolly pine chips. Tappi J. 70(1): 51–54.

VIA, B. K., T. F. SHUPE, L. H. GROOM, M. STINE, AND C. L. SO. 2003. Multivariate modeling of density, strength and stiffness from near infrared spectra for mature, juvenile and pith wood of longleaf pine (*Pinus palustris*). J. Near Infrared Spec. 11(5):365–378.

WÜLFERT, F. W. T. KOK, O. E. DE NOORD, AND A. K. SMILDE. 2000. Linear techniques to correct for temperature-induced spectral variation in multivariate calibration. Chemometr. Intell. Lab. 51(2):189–200.